

Study on the Relationship Between MRI Functional Imaging and Multiple Immunohistochemical Features of Glioma: A Noninvasive and More Precise Glioma Management

Molecular Imaging
Volume 23: 1–13
© The Author(s) 2024
Article reuse guidelines:
sagepub.com/journals-permissions
DOI: 10.1177/15353508241261583
journals.sagepub.com/home/mix



Jing Li, MD¹ , Jingtao Sun, BS¹, Ning Wang, MS² and Yan Zhang, MS³

Abstract

Objective: To investigate the performance of diffusion-tensor imaging (DTI) and hydrogen proton magnetic resonance spectroscopy (¹H-MRS) parameters in predicting the immunohistochemistry (IHC) biomarkers of glioma.

Methods: Patients with glioma confirmed by pathology from March 2015 to September 2019 were analyzed, the preoperative DTI and ¹H-MRS images were collected, apparent diffusion coefficient (ADC) and fractional anisotropy (FA), in the lesion area were measured, the relative values relative ADC (rADC) and relative FA (rFA) were obtained by the ratio of them in the lesion area to the contralateral normal area. The peak of each metabolite in the lesion area of ¹H-MRS image: N-acetylaspartate (NAA), choline (Cho), and creatine (Cr), and metabolite ratio: NAA/Cho, NAA/(Cho + Cr) were selected and calculated. The preoperative IHC data were collected including CD34, Ki-67, p53, S-100, syn, vimentin, NeuN, Nestin, and glial fibrillary acidic protein.

Results: One predicting parameter of DTI was screened, the rADC of the Ki-67 positive group was lower than that of the negative group. Two parameters of ¹H-MRS were found to have significant reference values for glioma grades, the NAA and Cr decreased as the grade of glioma increased, moreover, Ki-67 Li was negatively correlated with NAA and Cr.

Conclusion: NAA and Cr have potential application value in predicting glioma grades and tumor proliferation activity. Only rADC has predictive value for Ki-67 expression among DTI parameters.

Keywords

glioma, immunohistochemistry, diffusion tensor imaging, hydrogen proton magnetic resonance spectroscopy, biomarker

Received October 2, 2023; Revised May 9, 2024; Accepted for publication May 23, 2024

Introduction

Glioma is the most aggressive primary brain tumor with a poor prognosis and low survival.¹ According to the World Health Organization (WHO) grading system, it is divided into 4 pathological grades (I-IV),² namely, grades I and II are low-grade gliomas (LGGs), and grades III and IV are high-grade gliomas (HGGs). In 2016 and 2021, WHO updated the classification of glioma by combining molecular markers with histopathology, emphasizing the importance

¹Department of Radiology, Tangshan Women and Children's Hospital, Tangshan, Hebei, China

²Department of Radiology and Nuclear Medicine, The First Hospital of Hebei Medical University, Shijiazhuang, Hebei, China

³Department of Radiology, The Second Hospital of Hebei Medical University, Shijiazhuang, Hebei, China

Corresponding Author:

Jingtao Sun, Department of Radiology, Tangshan Women and Children's Hospital, No.1 Hetai Road, Tangshan, Hebei 063000, China.
Email: 1146932039@qq.com



Creative Commons Non Commercial CC BY-NC: This article is distributed under the terms of the Creative Commons Attribution-NonCommercial 4.0 License (<https://creativecommons.org/licenses/by-nc/4.0/>) which permits non-commercial use, reproduction and distribution of the work without further permission provided the original work is attributed as specified on the SAGE and Open Access page (<https://us.sagepub.com/en-us/nam/open-access-at-sage>).

of molecular detection.^{2,3} The fifth edition of the WHO Classification of central nervous system tumors (WHO CNS 5), published in 2021, has achieved substantial changes by further promoting the role of molecular diagnosis in CNS tumor classification but still rooted in other established methods of tumor characterization, including histology and immunohistochemistry (IHC).³ Among them, the expression of Ki-67, vimentin, CD34, S-100, p53, syn, and Glial Fibrillary Acidic Protein (GFAP) are important factors in judging and predicting the biological behavior of tumor cells.⁴⁻⁸ Recently, molecular biomarkers have become increasingly important in providing assistance and defining diagnostic information.

Diffusion-tensor imaging (DTI) is an *in vivo* functional imaging technology developed on the basis of diffusion-weighted imaging (DWI). It can comprehensively evaluate the diffusion movement of water molecules, the degree of compression, infiltration, and destruction of surrounding white matter fiber bundles from the microscopic perspective. Studies have shown that the apparent diffusion coefficient (ADC) and fractional anisotropy (FA) of the tumor have high application value in the differential diagnosis, grades, and the degree of white matter infiltration of glioma.^{9,10}

According to WHO CNS 5, in addition to major changes in the classification of glioma, it is important to provide information on the role of Hydrogen proton magnetic resonance spectroscopy (¹H-MRS) in glioma diagnosis, follow-up, and research.¹¹ ¹H-MRS is a proven technique for glioma diagnosis and follow-up in clinical practice. Tumor metabolite levels can be assessed, the main metabolites are N-acetylaspartate (NAA), choline (Cho), and creatine (Cr), NAA is a marker of neuronal activity, Cr is a cue for energy metabolism in brain tissue, and Cho is a marker of cell membrane synthesis. In glioma, the general rule is that NAA and Cr decrease with increasing tumor grade, while other metabolites increase. Cho/NAA quantitatively reflects tumor cell proliferation and local neuronal destruction without complex transitions.¹²

At present, only DTI and MRS parameters predicting Ki-67 Labeling Index (Ki-67 Li) tumor proliferation activity studies can be detected,¹³ while vimentin, CD34, S-100, p53, Syn, and GFAP have not been discussed yet. Therefore, this study was based on the predictive efficacy of 3 T ¹H-MRS and DTI parameters on glioma grades and IHC characteristics, in order to preliminarily explore the feasibility of ¹H-MRS and DTI parameters in predicting molecular typing of glioma.

Materials and Method

This retrospective study was according to the World Medical Association Declaration of Helsinki statement for research involving human subjects and was approved by the institutional ethics committee of the hospital (Research Ethics Committee of our Hospital. Approval No.2021-001-01) on

March 8, 2021. All patients signed informed consent for magnetic resonance imaging (MRI) safety examination before the MRI examination. All data were fully anonymized before we accessed them.

Population

WHO CNS 5 has changed all CNS WHO tumor grades to Arabic numerals: (1-4). Because CNS tumor grades correlate with overall expected clinical biological behavior, the WHO CNS 5 generally retains the grade ranges used for tumor types in previous versions, so in our study, the glioma grades I to IV promulgated by WHO in 2016 were still used.

A total of 77 patients with pathologically confirmed gliomas from March 2015 to September 2019 in the PACS system were retrospectively included. Among them, 57 cases had complete DTI parameters, including 31 males and 26 females, with an average age of (49.70 ± 14.05) years from 7 to 72 years. In the 57 patients, there were 57 Ki-67 IHC cases, 48 CD34 IHC cases, 48 S-100 IHC cases, 48 vimentin IHC cases, 36 syn IHC cases, and 29 p53 IHC cases, respectively. 28 cases had the nestin IHC test and 57 cases had the GFAP IHC test, they were all positive expressions, so nestin and GFAP were not included in the study. A total of 31 patients were tested for NeuN IHC (label 0-29 cases and label 1-2 cases), since the total weight of each case was < 5, the significance could not be calculated, so NeuN was not included. All IHC indicators were divided into label 0 group (negative expression ones) and label 1 group (positive expression ones). More information is listed in Table 1.

Among the above 57 cases, 42 cases had complete MRS parameters, including 25 males and 17 females, with an average age of (47.45 ± 13.96) from 7 to 71 years. In the 42 patients, there were 42 Ki-67 IHC cases, 35 CD34 IHC cases, 36 S-100 IHC cases, 36 vimentin IHC cases, 29 syn IHC cases, and 20 p53 IHC cases, respectively. All 42 patients underwent the GFAP IHC test, and as all of them were positive, it was not analyzed. A total of 22 cases underwent the Nestin IHC test (label 0-2 cases and label 1-20 cases), and 23 patients were tested for NeuN IHC (label 0-20 cases and label 1-3 cases), since the total weight of Nestin and NeuN was < 5, the significance could not be calculated, so no analysis was made. More information is listed in Table 1.

Inclusion criteria: Patients with glioma were diagnosed by histopathologic examination through surgery. Exclusion criteria: Intracranial decompression, chemotherapy, and radiotherapy were performed before the MRI examination. Artifacts appeared in the MRI images.

MRI Protocol

Philips 3.0 T MRI system and 8-channel orthogonal head coil were used. SE-EPI sequence was performed for DTI, and the scanning parameters were as follows: TR: 10 000 ms, TE was

Table 1. Demographic and Clinical Characteristics of Patients.

Characteristics	DTI group (n = 57)	MRS group (n = 42)
Age(mean ± SD, years)	49.70 ± 14.05	47.45 ± 13.96
Sex		
Male	31 (54%)	25 (60%)
Female	26 (46%)	17 (40%)
Grade		
WHO II	17 (30%)	17 (40%)
WHO III	22 (39%)	15 (36%)
WHO IV	18 (31%)	10 (24%)
Histologic characteristic		
Oligodendroglioma	10 (17.6%)	11 (26.2%)
Astrocytoma	3 (5.3%)	1 (2.4%)
Diffuse astrocytoma	2 (3.5%)	3 (7.1%)
Ganglioglioma	2 (3.5%)	2 (4.8%)
Anaplastic oligodendroglioma	6 (10.5%)	6 (14.3%)
Anaplastic astrocytoma	8 (14%)	5 (11.9%)
Anaplastic ependymoma	6 (10.5%)	3 (7.1%)
Anaplastic pleomorphic xanthoastrocytoma	2 (3.5%)	1 (2.4%)
Glioblastoma	18 (31.6%)	10 (23.8%)
Lesion location		
Frontal lobe	25	15
Temporal lobe	27	24
Parietal lobe	12	7
Occipital lobe	8	5
Insular lobe	7	7
Basal ganglia	2	2
Thalamus	2	1
Lateral ventricle	2	1
Corpus callosum	1	0
Ki-67		
Label 0	19 (33.3%)	17 (40.5%)
Label I	38 (66.7%)	25 (59.5%)
CD34		
Label 0	24 (50%)	21 (60%)
Label I	24 (50%)	14 (40%)
S-100		
Label 0	7 (14.6%)	6 (16.7%)
Label I	41 (85.4%)	30 (83.3%)
vimentin		
Label 0	7 (14.6%)	9 (25%)
Label I	41 (85.4%)	27 (75%)
p53		
Label 0	12 (41.4%)	7 (35%)
Label I	17 (58.6%)	13 (65%)
syn		
Label 0	17 (47.2%)	15 (51.7%)
Label I	19 (52.8%)	14 (48.3%)

Abbreviations: DTI, diffusion tensor imaging; MRS, magnetic resonance spectroscopy; WHO, World Health Organization.

the smallest. ¹H-MRS acquisition parameters: Chemical shift imaging (CSI) point resolved spectrum (2d_press_144 fast sense), TR = 1500 ms TE = 144 ms Voxel size = 10 mm × 10 mm, FOV = 80 mm × 110 mm.

Immunohistochemical status

All patients in this study underwent surgical resection of glioma. IHC staining was performed on formalin-fixed and paraffin-embedded sections of brain tumor resected specimens. The expressions of Ki-67, vimentin, CD34, S-100, p53, syn, and GFAP in glioma were detected by SP staining with benchmark GX automatic IHC (Figure 1). The rate of Ki-67 Li < 20% was classified as negative and ≥ 20% as positive,¹⁴ and the cell proliferation index was measured with IHC analysis by using the rabbit anti-human monoclonal antibody against the Ki-67 protein. IHC indicators were classified as negative and positive which were represented by 0, 1. IHC staining results were evaluated by 2 pathologists.

Data Labeling and Measurement

DTI parameter measurement (Figure 2): DTI used the continuous fiber tract tracing method. In the lesion area, the ADC, FA, and fiber bundle length were measured, and the relative values rADC, rFA, and rlength were obtained by the ratio of ADC, and FA values in the lesion area to the contralateral normal brain area.

The lesion area of the MRS image was selected, and the metabolite peak and the metabolite ratio were calculated (Figure 3). Regions of interest (ROIs) were delineated on the solid parts of each tumor center, ROIs on necrotic areas, cystic intertumoral areas, and areas of presumed perilesional vasogenic edema were excluded from the analysis. We selected NAA, Cho, Cr, NAA/Cho, and NAA/(Cho + Cr).

Among all participants, a consensus was reached between a radiologist (with 10 years of experience in radiology) and a technologist (with 5 + years of experience in MRI procedures).

Statistical Analysis

IBM SPSS Statistics.22 was used for statistical analysis. It was used to test the normality (Kolmogorov Smirnov, $P > .05$) and the homogeneity of variance (Levene test, $P > .05$) of continuous variables in the clinic, 2-independent sample t -test (meeting the normality and homogeneity of variance test) was conducted to compare the distribution differences between the 2 groups, approximate t -test was applied when equal variances not assumed, rank sum test (Mann-Whitney nonparametric test) was performed when the quantitative data were skewed. Analysis of variance (F -test) was selected to compare the mean of 3 sample groups, and the Kruskal-Wallis Test (χ^2) was used for unequal variances. The correlation between the Ki-67 Li and DTI, MRS parameters were evaluated with the Pearson correlation coefficient, and the Spearman correlation coefficient was selected as the data with bivariate non-normal distribution. $P < .05$ was statistically significant.

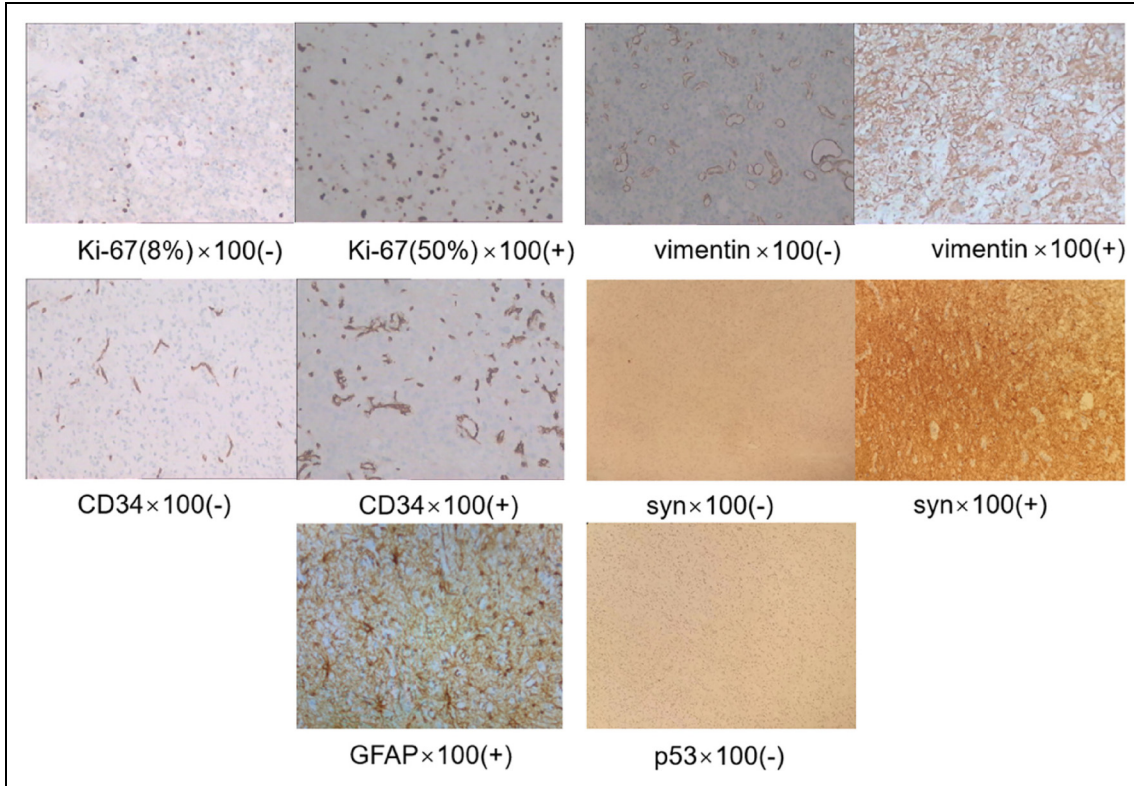


Figure 1. Immunohistochemistry of positive and negative staining (100 \times).

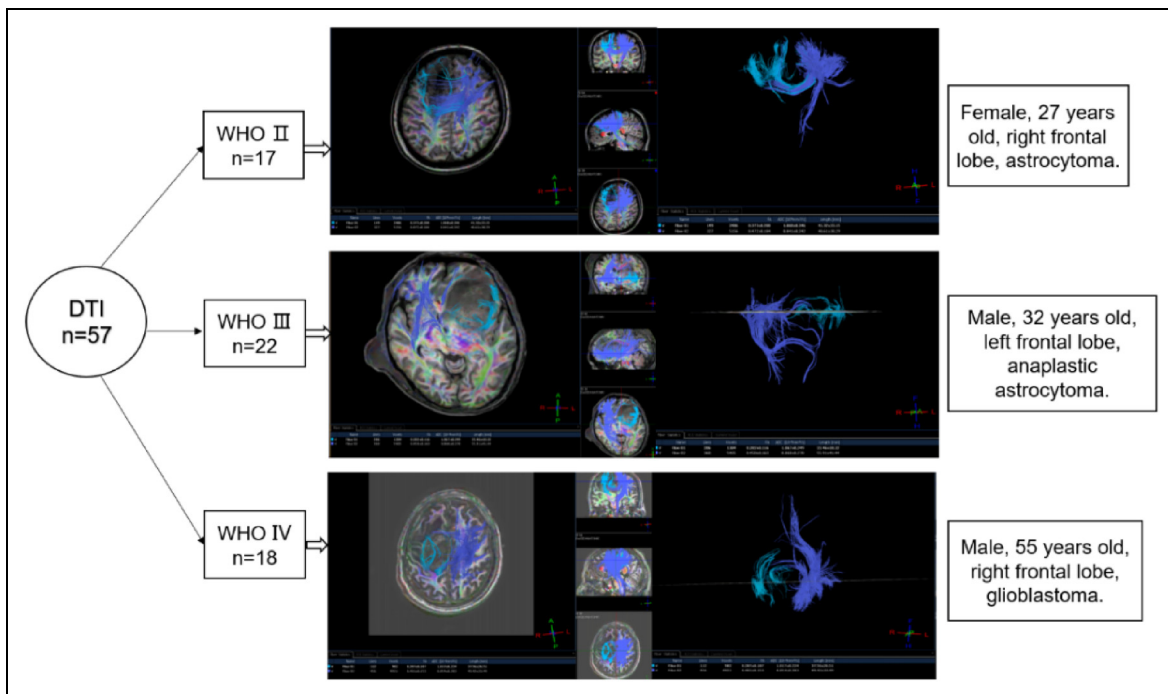


Figure 2. Collection of diffusion tensor imaging (DTI) patients.

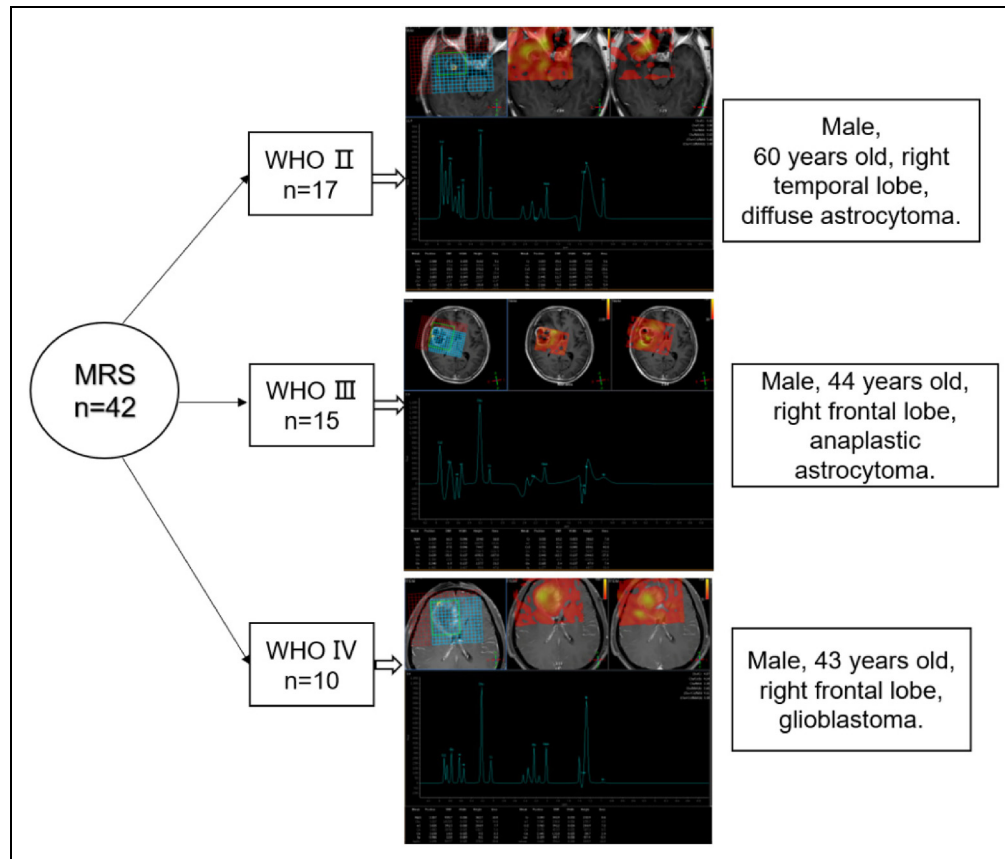


Figure 3. Collection of magnetic resonance spectroscopy (MRS) patients.

Results

The Relationship Between DTI Parameters and the Negative and Positive of IHC Indicators

The relationship between DTI-specific parameters ADC, AA, rADC, rFA, rlength, and Ki-67, CD34, S-100, vimentin, p53, and syn was selected, respectively, only the rADC of the Ki-67 positive group was lower than that in negative ones ($Z = -1.947$, $P = .052$), this indicates that increased cell density tends to occur in voxels with lower ADC values. The rlength in Ki-67, CD34, S-100, and p53 positive groups were lower than those in negative ones, it shows that the damage of fiber bundles in Ki-67, CD34, S-100, and p53 positive cases is slightly more serious than that in negative ones however, there were no statistical differences. Although the ADC in the p53 positive group was higher than that in negative ones, the difference was not statistically significant (Table 2).

The Relationship among DTI Parameters and Glioma Grades

There was no significant difference among DTI-specific parameters ADC, FA, rADC, rFA, rlength, and glioma grades (Table 3).

Correlation Between Glioma Proliferation Index Ki67 Li and DTI Parameters

There was no correlation between Ki-67 Li and DTI parameters FA, ADC, rFA, rADC, but rADC decreased with Ki-67 Li increasing ($r = -0.239$, $P = .073$), and rFA increased while Ki-67 Li increasing ($r = 0.230$, $P = .086$) (Figure 3).

MRS Parameter Kurtosis in Differentiating Negative to Positive IHC Indicators

The MRS parameters NAA, Cho, Cr, NAA/Cho, and NAA/(Cho + Cr) were not related to Ki-67, CD34, S-100, vimentin, p53, and syn (Table 4).

The Relationship Between MRS Parameters and Glioma Grades

The difference in NAA among WHO II, III, and IV grades of glioma was statistically significant ($F = 3.257$, $P = .049$), and the NAA decreased with the increased glioma grades. The difference in Cr among WHO II, III, and IV grades of glioma was statistically significant ($F = 4.948$, $P = 0.012$), with the increased grades, the value of Cr decreased.

Table 2. The Relationship Between DTI Parameters and the Negative and Positive of IHC Indicators.

		ABADC ($10^3 \text{ mm}^2/\text{s}$)	ABFA	rADC ($10^3 \text{ mm}^2/\text{s}$)	rFA	rlength (mm)
Ki-67	Label 0 (n = 19)	1.102 ± 0.087	0.322 ± 0.044	1.281 ± 0.145	0.753 ± 0.086	0.759 ± 0.183
	Label 1 (n = 38)	1.083 ± 0.155 F = 8.307, P = .006 t = -0.585, P = .561	0.326 ± 0.070 F = 4.161, P = .046 t = -0.296, P = .768	1.222 ± 0.184 Z = -1.947, P = .052	0.768 ± 0.129 F = 5.102, P = .028 t = -0.526, P = .601	0.733 ± 0.191 F = 0.011, P = .918 t = -0.493, P = .624
CD34	Label 0 (n = 24)	1.078 ± 0.142	0.315 ± 0.061	1.244 ± 0.178	0.750 ± 0.112	0.774 ± 0.171
	Label 1 (n = 24)	1.122 ± 0.121 F = 0.143, P = .707 t = -1.145, P = .258	0.324 ± 0.062 F = 0.004, P = .952 t = -0.562, P = .577	1.267 ± 0.163 Z = -0.474, P = .635	0.754 ± 0.124 F = 1.185, P = .282 t = -0.143, P = .887	0.685 ± 0.187 F = 0.73, P = .397 t = 1.729, P = .091
S-100	Label 0 (n = 7)	1.072 ± 0.158	0.312 ± 0.049	1.265 ± 0.195	0.751 ± 0.123	0.789 ± 0.204
	Label 1 (n = 41)	1.102 ± 0.130 F = 0.001, P = .975 t = -0.484, P = .643	0.317 ± 0.056 F = 0.043, P = .836 t = -0.229, P = .820	1.263 ± 0.171 F = 0.017, P = 0.898 t = 0.034, P = .973	0.752 ± 0.118 F = 0.044, P = 0.835 t = -0.015, P = .988	0.721 ± 0.187 F = 0.283, P = 0.597 t = 0.882, P = .383
vimentin	Label 0 (n = 7)	1.101 ± 0.100	0.308 ± 0.035	1.216 ± 0.071	0.777 ± 0.084	0.722 ± 0.186
	Label 1 (n = 41)	1.087 ± 0.143 F = 1.006, P = .321 t = 0.247, P = .806	0.323 ± 0.063 F = 1.757, P = .191 t = -0.607, P = .547	1.248 ± 0.191 F = 3.943, P = .053 t = -0.425, P = .673	0.760 ± 0.123 Z = -0.453, P = .668	0.734 ± 0.176 F = 0.004, P = .949 t = -0.164, P = .871
p53	Label 0 (n = 12)	1.051 ± 0.134	0.343 ± 0.073	1.234 ± 0.175	0.791 ± 0.118	0.764 ± 0.213
	Label 1 (n = 17)	1.145 ± 0.138 F = 0.134, P = .717 t = -1.825, P = .079	0.316 ± 0.065 F = 0.030, P = .865 t = 1.065, P = .296	1.302 ± 0.203 F = 0.432, P = .517 t = -0.937, P = .357	0.748 ± 0.134 F = 0.116, P = .736 t = 0.901, P = .376	0.721 ± 0.187 F = 0.294, P = .592 t = 0.569, P = .574
syn	Label 0 (n = 17)	1.094 ± 0.146	0.329 ± 0.070	1.247 ± 0.176	0.777 ± 0.124	0.716 ± 0.166
	Label 1 (n = 19)	1.108 ± 0.106 F = 1.872, P = .180 t = -0.317, P = .753	0.314 ± 0.053 F = 1.390, P = .247 t = 0.749, P = .459	1.275 ± 0.148 F = 0.482, P = .492 t = -0.532, P = .598	0.748 ± 0.096 F = 1.794, P = .189 t = 0.801, P = .428	0.726 ± 0.188 F = 0.250, P = .620 t = -0.172, P = .864

Abbreviations: IHC, immunohistochemistry; DTI, diffusion tensor imaging; ADC, apparent diffusion coefficient; rADC, relative apparent diffusion coefficient; rFA, relative fractional anisotropy; rlength, relative length.

Table 3. The Relationship Among DTI Parameters and Glioma Grade.

	ABADC ($10^3 \text{ mm}^2/\text{s}$)	ABFA	rADC	rFA	rlength (mm)
WHO II (n = 17)	1.111 \pm 0.090	0.309 \pm 0.035	1.279 \pm 0.145	0.747 \pm 0.076	0.734 \pm 0.197
WHO III (n = 22)	1.058 \pm 0.149	0.349 \pm 0.071	1.197 \pm 0.169	0.777 \pm 0.125	0.742 \pm 0.195
WHO IV (n = 18)	1.108 \pm 0.154	0.310 \pm 0.064	1.261 \pm 0.198	0.762 \pm 0.137	0.747 \pm 0.179
	$F = 0.986, P = .380$	$\chi^2 = 4.697, P = .095$	$\chi^2 = 2.596, P = .273$	$\chi^2 = 0.833, P = .659$	$F = 0.020, P = .981$

Abbreviations: WHO, World Health Organization; DTI, diffusion tensor imaging; ADC, apparent diffusion coefficient; rADC, relative apparent diffusion coefficient; rFA, relative fractional anisotropy; rlength, relative length.

However, there was no significant difference between Cho, NAA/Cho, NAA/(Cho + Cr), and glioma grades (Table 5).

We selected the average value of Cr in WHO III as the reference value and calculated the specificity and sensitivity in predicting the grade of glioma, they are 75.0% and 61.1%, respectively, Cr has a relatively high specificity and low sensitivity in distinguishing the glioma grades. The selection of the cut-off point of Cr was related to it (Table 6).

Correlation Between Ki-67 Li and MRS Parameters

Ki-67 Li was negatively correlated with NAA ($r = -0.322, P = .037$), and the NAA decreased with Ki-67 Li increasing. Ki-67 Li was negatively correlated with Cr ($r = -0.305, P = .050$), and the Cr decreased with the increased Ki-67 Li. There was no correlation between Ki-67 Li and Cho, NAA/Cho, and NAA/(Cho + Cr) (Figure 4). This suggests that the proposed parameters NAA, and Cr may provide an effective tool to identify tumors with high proliferative activity (Figure 5).

Discussion

At present, there are sufficient studies showing that gliomas with the same or similar histological features may carry different molecular or genetic information.³ As a biomarker of cell proliferation, Ki-67 has been incorporated into the grade and prognosis prediction of CNS tumors.¹⁵ CD34 is a transmembrane phosphoglycoprotein, first discovered in hematopoietic stem and progenitor cells, it is known as the best marker for microvessel density studies and plays a crucial role in the regulation of glioma angiogenesis, CD34 overexpression is associated with higher-grade gliomas and can serve as a potential glioma diagnostic and prognostic marker, as well as a useful therapeutic target.¹⁶ Pleomorphic low-grade neuroepithelial tumor of the young (PLNTY) is a glioma associated with a history of epilepsy in youth, a diffuse growth pattern, frequent oligodendroglioma-like components, calcification, CD34 immunoreactivity, and the MAPK pathway, CD34 immunostaining was often intense and diffuse in the tumor.³ Vimentin is an intermediate filament family protein that maintains cell integrity and participates in multiple cell signaling pathways to regulate cancer cell motility and invasion, and it is an independent important prognostic

factor in patients with high-grade gliomas.¹⁷ S-100 protein¹⁸ named for its solubility in saturated ammonium sulfate, is derived from brain tissue, is a dimer, and belongs to the thermolabile acidic calcium-binding protein. It is present in gliomas, but its amount varies with the histological type of the tumor, mostly in ependymomas, it is also present in schwannomas and neurofibromas, but not in neuronal-derived in tumors such as medulloblastoma and neuroblastoma. A recent study showed¹⁹ that p53-IHC should be used as a complement to the morphological diagnosis of H&E and that p53-IHC diffuse or strong positivity is sufficient to diagnose astrocytoma without 1p/19q testing, and the mutational status of p53 is correlated with IHC, there appears to be an incomplete parallel between the results. Syn is synaptophysin, mainly present in neuron neuroendocrine cells in presynaptic vesicles of neurons, and this antibody is mainly used to label neuroendocrine cells and their tumors.²⁰ GFAP is almost exclusively expressed in astrocytes,²¹ and all cases in this study were positive for GFAP, so it could not be used for dichotomous studies. Therefore, fully considering the molecular pathological characteristics of glioma can help to determine the heterogeneity and prognosis of glioma.²²

In the research of Figini et al,²³ they pointed out that diffusion MRI has the potential to provide such in vivo indicators. It provides easy access to the microstructure of the whole tumor at a rather high spatial resolution. DTI is the most often utilized approach nowadays.²⁴ ADC and FA are DTI indices that correspond with changes in cellular density and extracellular matrix characteristics caused by glioma invasion and proliferation. FA was substantially greater in grade II and III isocitrate dehydrogenase (IDH) wild-type gliomas than in IDH mutant gliomas.²³ The present study demonstrates that the DTI parameter rADC has a predictive value for the negative and positive of IHC marker Ki-67, although the rlength value in Ki-67, CD34, S-100, and p53 positive groups was lower than in negative ones, the ABADC value of p53-positive cases was higher than that of negative ones, but unfortunately the difference was not statistically significant. The interpretation of DTI results in clinical work was divided into 2 aspects. On the one hand, the lesions were directly observed through the ADC map and FA map calculated by DTI. On the other hand, the lesions were quantitatively evaluated by measuring parameters such as ADC and FA values of different grades of

Table 4. MRS Parameter Kurtosis in Differentiating Negative to Positive of IHC Indicators.

	NAA	Cho	Cr	NAA/Cho	NAA/(Cho + Cr)
Ki-67	Label 0 (n = 17)	2067.794 ± 969.803	834.524 ± 442.816	0.289 ± 0.160	0.200 ± 0.104
	Label 1 (n = 25)	1604.636 ± 1033.605	532.812 ± 426.892	0.297 ± 0.210	0.210 ± 0.118
	Z = -1.602, P = .109	Z = -1.794, P = .073	Z = -2.601, P = .009	Z = -0.218, P = .828	F = 0.078, P = .782 t = -0.270, P = .788 0.214 ± 0.132
CD34	Label 0 (n = 21)	1611.390 ± 880.278	560.976 ± 422.250	0.310 ± 0.237	0.218 ± 0.089
	Label 1 (n = 14)	1476.343 ± 920.707	507.521 ± 273.773	0.302 ± 0.131	F = 1.420, P = .242
	Z = -0.168, P = .866	F = 0.498, P = .485 t = -0.437, P = .665	Z = 0.000, P = 1.000	Z = -0.455, P = .649	t = -0.075, P = .941
S-100	Label 0 (n = 6)	593.067 ± 496.776	889.367 ± 627.581	0.311 ± 0.177	0.209 ± 0.103
	Label 1 (n = 30)	399.073 ± 211.597	576.763 ± 369.620	0.286 ± 0.199	0.199 ± 0.112
	F = 8.766, P = 0.006 t = 0.940, P = .388	F = 0.155, P = .696 t = 0.444, P = .660	F = 2.657, P = .112 t = 1.674, P = 0.103	Z = -0.552, P = .581	Z = -0.340, P = .734
vimentin	Label 0 (n = 9)	508.733 ± 277.633	739.111 ± 446.792	0.393 ± 0.309	0.252 ± 0.159
	Label 1 (n = 27)	467.022 ± 288.589	631.415 ± 420.278	0.289 ± 0.135	0.208 ± 0.094
	F = 0.111, P = .741	F = 1.144, P = .292	F = 0.026, P = .873	F = 3.795, P = .060	F = 1.761, P = .193
p53	Label 0 (n = 7)	439.857 ± 228.568	1527.029 ± 795.185	t = -0.656, P = .516	t = 1.028, P = .311
	Label 1 (n = 13)	353.977 ± 204.027	1682.946 ± 984.366	670.014 ± 375.729	0.212 ± 0.099
	F = 0.187, P = .670	F = 0.828, P = .375	518.485 ± 318.558	0.250 ± 0.112	0.186 ± 0.089
syn	Label 0 (n = 15)	349.513 ± 182.103	1760.220 ± 1016.922	F = 0.033, P = .859	F = 0.059, P = .811
	Label 1 (n = 14)	567.157 ± 361.450	1748.179 ± 1052.868	t = -0.954, P = .353	t = 0.602, P = .555
	F = 5.496, P = .027 t = -2.026, P = .057	F = 0.008, P = .929 t = 0.031, P = .975	791.493 ± 543.956	t = 0.984, P = .338	0.181 ± 0.134
			F = 1.037, P = .318	0.358 ± 0.160	0.249 ± 0.109
			t = -1.254, P = .221	Z = -2.313, P = .021	Z = -2.096, P = .036

Abbreviations: MRS, magnetic resonance spectroscopy; IHC, immunohistochemistry; Cr, creatine; NAA, N-acetylaspartate; Cho, choline.

Table 5. The Relationship Between MRS Parameters and Glioma Grades.

	NAA	Cho	Cr	NAA/Cho	NAA/(Cho + Cr)
WHO II (n = 17)	558.400 ± 334.509	1986.235 ± 1107.085	871.253 ± 521.838	0.351 ± 0.255	0.230 ± 0.140
WHO III (n = 15)	426.060 ± 210.713	1895.687 ± 967.079	607.187 ± 341.243	0.251 ± 0.129	0.186 ± 0.089
WHO IV (n = 10)	298.010 ± 155.676	1306.710 ± 881.782	358.810 ± 286.419	0.259 ± 0.105	0.196 ± 0.087
	$F = 3.257, P = .049$	$\chi^2 = 3.916, P = .141$	$F = 4.948, P = .012$	$F = 1.353, P = .270$	$F = 0.646, P = .529$

Abbreviations: MRS, magnetic resonance spectroscopy; WHO, World Health Organization; Cr, creatine; NAA, N-acetylaspartate; Cho, choline.

Table 6. The Relationship Between MRS Parameter Cr and Glioma Grades.

MRS parameter	WHO II (n)	True positive (n)	False positive (n)	WHO III and IV (n)	True negative (n)	False negative (n)	Specificity (%)	Sensitivity (%)
Cr ≥ 607	17	11	6	25	19	6	75.0	61.1

Abbreviations: MRS, magnetic resonance spectroscopy; Cr, creatine; WHO, World Health Organization.

glioma, and the overall ADC and FA values were obtained by the fiber tract tracing method, which reflected the destruction of the fiber bundles in the brain tissue by the tumor. But there is disagreement about the interpretation of ADC changes in DWI-derived brain tumors, it has been reported that restricted spread was affected not only by tumor cell density and metabolic activity, but also by other factors, such as ischemia or compression, in addition, DWI-derived ADCs were sensitive to other tissue characteristics, including due to vasogenic edema or extracellular fluid arising from the tumor-induced disruption of extracellular structures.²⁵ Due to the poor display of glioma lesions on the ADC and FA maps, our study did not choose to outline the lesion contour on the ADC and FA maps to extract image features. Instead, DTI used a continuous fiber tract tracing method, and quantitative indicators such as ADC, FA, and other values of the target lesion were measured. The results of this study showed that the measurement of DTI quantitative indicators only rADC could be used for the prediction of glioma IHC, this indicates that increased cell density tends to occur in voxels with lower ADC values. A recent retrospective DTI study has stratified LGG according to IDH and 1p/19q status. They reported that IDH wild-type astrocytoma and oligodendroglioma had lower ADC and higher FA, but there was no significant difference between glioma with and without 1p/19q deletion.^{26–28}

In our study, DTI parameters failed to predict the grade of glioma. No correlation was found between Ki-67 Li and DTI parameters such as ABFA, ABADC, rFA, and rADC, but rADC decreased with the increased Ki-67 Li, and rFA increased with the increased Ki-67 Li. Similar studies suggested that some features of FA may be helpful in distinguishing LGG from HGG.^{29,30} There were also studies that showed that FA played no role in differentiating glioma grades.³¹

Preoperative grade of glioma based on conventional MRI can be difficult, especially in the absence of significant edema

and/or contrast enhancement. This is a common diagnostic challenge, even in high-grade tumors. In cases of uncertain diagnosis, more information can be obtained with MRS.³² Currently, optimized ¹H-MRS can noninvasively detect 2-hydroxyglutarate, a specific metabolite of IDH gene mutation.¹² Our results did not find that the MRS parameters NAA, Cho, Cr, NAA/Cho, NAA/(Cho + Cr) could differentiate Ki-67, CD34, S-100, vimentin, p53, and syn negative to positive. However, our study showed that NAA and Cr could provide a better differentiation between grades of glioma by the estimation of tumor cellularity. Correlation of Ki-67 Li with MRS parameters using Pearson's correlations in order to assess which parameters could predict tumor proliferative activity, Ki-67 Li was negatively correlated with NAA and Cr, this suggests that NAA, Cr may provide an effective tool to identify tumors with high proliferative activity. Our study demonstrated that NAA and Cr were promising imaging modalities for the noninvasive estimation of glioma grades and proliferative activity. Moreover, we selected the average value of Cr in WHO III as the reference value, Cr has a relatively high specificity in distinguishing the glioma grades. It has been reported that the most important metabolite that differentiated tumor progression (TP) from radiation-induced pseudoprogression (PSP) was Cho, however, Cr was not considered to be affected by radiation damage. Thus, in brain tissue undergoing radiation necrosis, an increased Cho/Cr ratio was observed.³³ It would be fascinating to investigate the potential of ¹H-MRS in the preoperative assessment of several molecular markers, as well as the ability of this approach to predict progression. The approach might be useful in differentiating distinct subtypes of glioma regarding the 2021 WHO Classification of CNS tumors.

There are several potential limitations in this study. The main limitation of this study is the small sample size and not doing power analysis for sample size calculation.

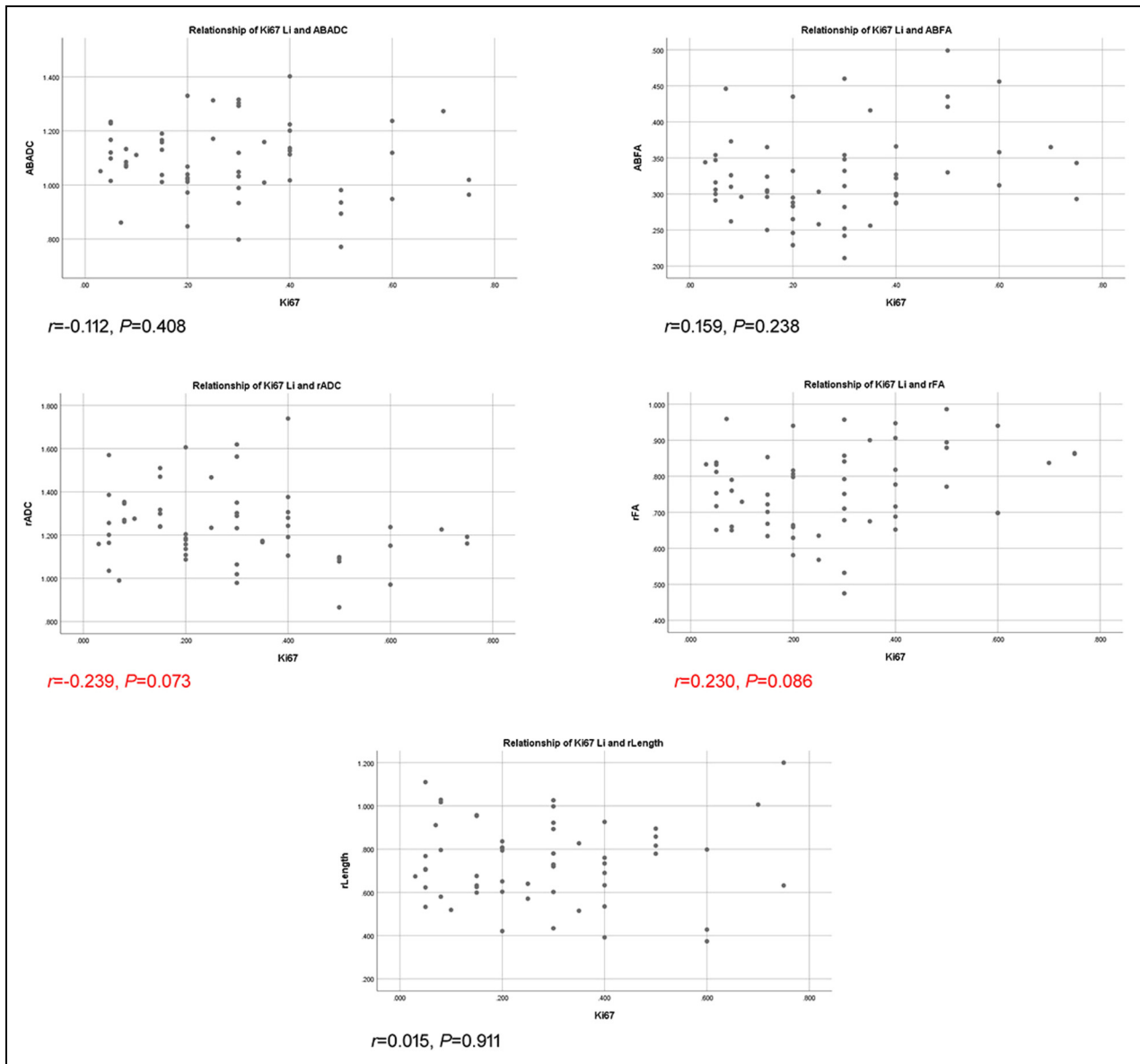


Figure 4. A scatter plot of the relationship between Ki-67 Li and DTI parameters. Abbreviations: DTI, diffusion tensor imaging; Ki-67 Li, Ki-67 labeling index.

Secondly, since DTI and MRS characterize different tumor characteristics, the 2 imaging modalities may also provide complementary information in the pretreatment evaluation of gliomas, in the current study, we focused on evaluating IHC protein markers, and further research could assess genotyping to determine whether they would provide additional clinically useful information in glioma evaluation. In addition, not all patients were tested for all of the above IHC indicators. Therefore, future studies should validate the findings of this study in a larger cohort with detailed pathology. An innovation of our study is that it combined the quantitative parameters of DTI and MRS to identify or predict IHC indicators, and maximized the

value of MR research for preoperative pathological grading of gliomas.

Conclusions

Overall, the present study demonstrates that the DTI parameter rADC has predictive value for the negative and positive of Ki-67 in glioma, and the MRS parameters NAA and Cr have potential application value for predicting the grade of glioma and tumor proliferative activity. However, there was no statistically significant difference between the other DTI parameters as well as all MRS parameters and the multiple IHC features of glioma. Meanwhile, DTI parameters could not predict the glioma grades in our study.

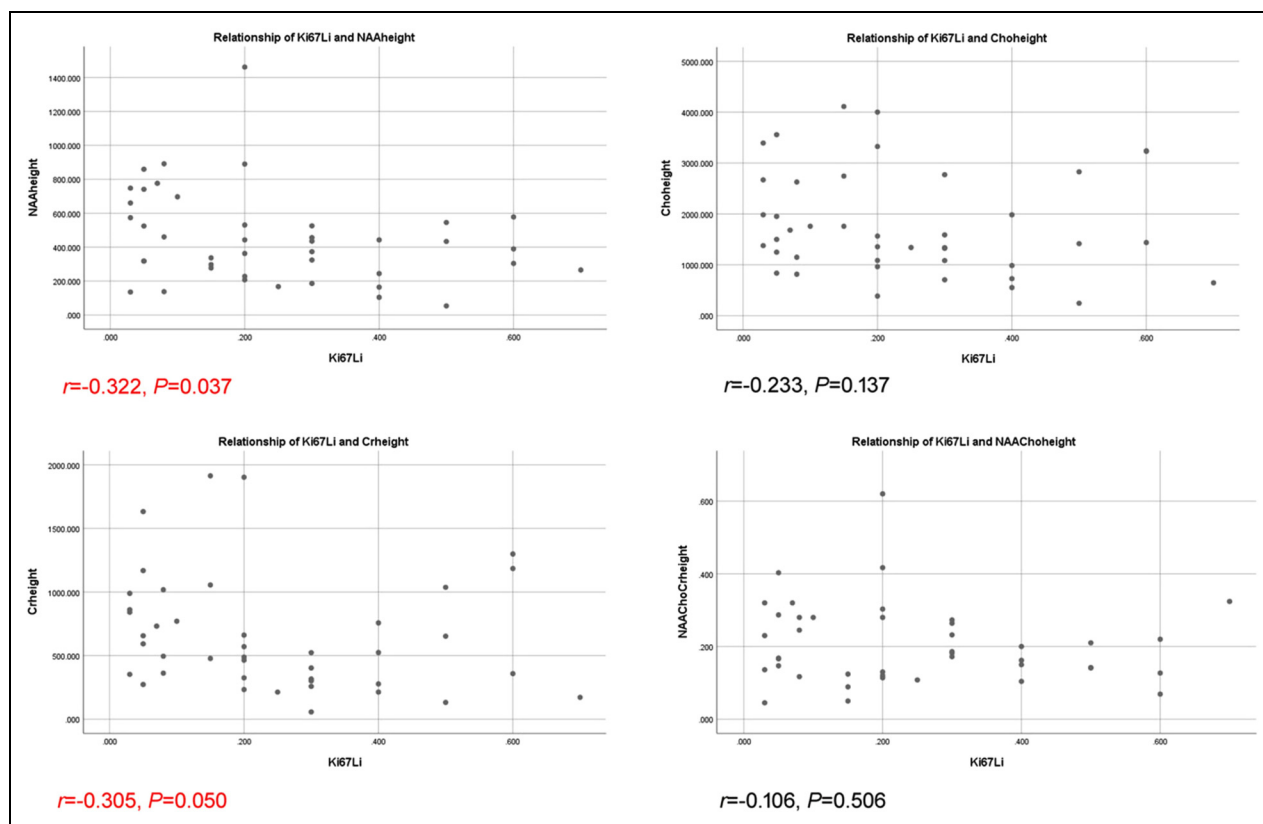


Figure 5. A scatter plot of the relationship between Ki-67 Li and MRS parameters. Abbreviations: MRS, magnetic resonance spectroscopy; Ki-67 Li, Ki-67 labeling index.

Abbreviations

MRI	magnetic resonance imaging
LGG	low-grade gliomas
HGG	high-grade glioma
WHO	World Health Organization
CNS	central nervous system
IHC	immunohistochemistry
DTI	diffusion tensor imaging
DWI	diffusion weighted imaging
ADC	apparent diffusion coefficient
FA	fractional anisotropy
¹ H-MRS	hydrogen proton magnetic resonance spectroscopy
NAA	N-acetylaspartate
Cho	choline
Cr	creatine
Ki-67 Li	Ki-67 labeling index
GFAP	glial fibrillary acidic protein
rADC	relative ADC
rFA	relative FA
rlength	relative length
CSI	chemical shift imaging
ROIs	regions of interest

PLNTY	pleomorphic low-grade neuroepithelial tumor of the young
IDH	isocitrate dehydrogenase
TP	tumor progression
PSP	radiation-induced pseudoprogession

Acknowledgments

We appreciate Professor Huaijun Liu's guidance and help.

Declaration of Conflicting Interests

The author(s) declared no potential conflicts of interest with respect to the research, authorship, and/or publication of this article.


Funding

The author(s) received no financial support for the research, authorship, and/or publication of this article.

Ethical Approval

The study was approved by the institutional ethics committee of the hospital (Research Ethics Committee of our Hospital. Approval No. 2021-001-01) on March 8, 2021. All patients signed informed consent for an MRI safety examination before the MRI examination. All data were fully anonymized before we accessed them.

ORCID iD

Jing Li  <https://orcid.org/0000-0003-0241-842X>

Supplemental material

Supplemental material for this article is available online.

References

- Vamvakas A, Williams SC, Theodorou K, et al. Imaging biomarker analysis of advanced multiparametric MRI for glioma grading. *Phys Med*. 2019;60:188–198. doi:10.1016/j.ejpm.2019.03.014 PMID: 30910431
- Louis DN, Perry A, Reifenberger G, et al. The 2016 World Health Organization classification of tumors of the central nervous system: a summary. *Acta Neuropathol*. 2016;131(6):803–820. doi:10.1007/s00401-016-1545-1 PMID:27157931
- Louis DN, Perry A, Wesseling P, et al. The 2021 WHO classification of tumors of the central nervous system: a summary. *Neuro Oncol*. 2021;23(8):1231–1251. doi:10.1093/neuonc/noab106 PMID:34185076
- Lin L, Wang G, Ming J, et al. Analysis of expression and prognostic significance of vimentin and the response to temozolomide in glioma patients. *Tumor Biol*. 2016;37(11):15333–15339. doi:10.1007/s13277-016-5462-7 PMID:27704357
- Nagaishi M, Yokoo H, Nobusawa S, et al. A distinctive pediatric case of low-grade glioma with extensive expression of CD34. *Brain Tumor Pathol*. 2016;33(1):71–74. doi:10.1007/s10014-015-0236-2 PMID:26496909
- Gates EDH, Lin JS, Weinberg JS, et al. Guiding the first biopsy in glioma patients using estimated Ki67 maps derived from MRI: conventional versus advanced imaging. *Neuro Oncol*. 2019;21(4):527–536. doi:10.1093/neuonc/noz004 PMID:30657997
- Van Eldik LJ, Zimmer DB. Secretion of S-100 from rat C6 glioma cells. *Brain Res*. 1987;436(2):367–370. doi:10.1016/0006-8993(87)91681-7 PMID:3435834
- Gillet E, Alentorn A, Doukouré B, et al. TP53 and p53 statuses and their clinical impact in diffuse low grade gliomas. *J Neurooncol*. 2014;118(1):131–139. doi:10.1007/s11060-014-1407-4 PMID:24590827
- Zhang Z, Xiao J, Wu S, et al. Deep convolutional radiomic features on diffusion tensor images for classification of glioma grades. *J Digit Imaging*. 2020;33(4):826–837. doi:10.1007/s10278-020-00322-4 PMID:32040669
- Figini M, Riva M, Graham M, et al. Prediction of isocitrate dehydrogenase genotype in brain gliomas with MRI: single-shell versus multishell diffusion models. *Radiology*. 2018;289(3):788–796. doi:10.1148/radiol.2018180054 PMID:30277427
- Galijasevic M, Steiger R, Mangesius S, et al. Magnetic resonance spectroscopy in diagnosis and follow-up of gliomas: state-of-the-art. *Cancers*. 2022;14(13):3197. doi:10.3390/cancers14133197
- Lin K, Cidan W, Qi Y, Wang X. Glioma grading prediction using multiparametric magnetic resonance imaging-based radiomics combined with proton magnetic resonance spectroscopy and diffusion tensor imaging. *Med Phys*. 2022;49(7):4419–4429. doi:10.1002/mp.15648 PMID:35366379
- Alexiou GA, Zikou A, Tsiouris S, et al. Correlation of diffusion tensor, dynamic susceptibility contrast MRI and (99 m) Tc-tetrofosmin brain SPECT with tumour grade and Ki-67 immunohistochemistry in glioma. *Clin Neurol Neurosurg*. 2014;116:41–45. doi:10.1016/j.clineuro.2013.11.003 PMID:24309151
- Panzuto F, Boninsegna L, Fazio N, et al. Metastatic and locally advanced pancreatic endocrine carcinomas: analysis of factors associated with disease progression. *J Clin Oncol*. 2011;29(17):2372–2377. doi:10.1200/JCO.2010.33.0688 PMID:21555696
- Chen WJ, He DS, Tang RX, Ren FH, Chen G. Ki-67 is a valuable prognostic factor in gliomas: evidence from a systematic review and meta-analysis. *Asian Pac J Cancer Prev*. 2015;16(2):411–420. doi:10.7314/apjcp.2015.16.2.411 PMID:25684464
- Kong X, Guan J, Ma W, et al. CD34 over-expression is associated with gliomas' higher WHO grade. *Medicine*. 2016;95(7):e2830. doi:10.1097/MD.0000000000002830 PMID:26886640
- Kim SI, Lee K, Bae J, et al. Revisiting vimentin: a negative surrogate marker of molecularly defined oligodendroglioma in adult type diffuse glioma. *Brain Tumor Pathol*. 2021;38(4):271–282. doi:10.1007/s10014-021-00411-4 PMID:34338912
- Cochran AJ, Wen DR. S-100 protein as a marker for melanocytic and other tumours. *Pathology*. 1985;17(2):340–345. doi:10.3109/00313028509063777 PMID:2995906
- Nishikawa T, Watanabe R, Kitano Y, et al. Reliability of IDH1-R132H and ATRX and/or p53 immunohistochemistry for molecular subclassification of Grade 2/3 gliomas. *Brain Tumor Pathol*. 2022;39(1):14–24. doi:10.1007/s10014-021-00418-x PMID:34826036
- Dong Y, Li Y, Liu R, et al. Secretagogin, a marker for neuroendocrine cells, is more sensitive and specific in large cell neuroendocrine carcinoma compared with the markers CD56, CgA, syn and Napsin A. *Oncol Lett*. 2020;19(3):2223–2230. doi:10.3892/ol.2020.11336 PMID:32194720
- Kiviniemi A, Gardberg M, Frantzén J, et al. Serum levels of GFAP and EGFR in primary and recurrent high-grade gliomas: correlation to tumor volume, molecular markers, and progression-free survival. *J Neurooncol*. 2015;124(2):237–245. doi:10.1007/s11060-015-1829-7 PMID:26033547
- Li J, Liu SY, Qin Y, et al. High-order radiomics features based on T2 FLAIR MRI predict multiple glioma immunohistochemical features: a more precise and personalized gliomas management. *PLoS One*. 2020;15(1):e0227703. doi:10.1371/journal.pone.0227703
- Figini M, Riva M, Graham M, et al. Prediction of isocitrate dehydrogenase genotype in brain gliomas with MRI: single-shell versus multishell diffusion models. *Radiology*. 2018;289(3):788–796. doi:10.1148/radiol.2018180054 PMID:30277427
- Basser PJ, Mattiello J, LeBihan D. MR diffusion tensor spectroscopy and imaging. *Biophys J*. 1994;66(1):259–267. doi:10.1016/S0006-3495(94)80775-1 PMID:8130344
- Jeong JW, Juhász C, Mittal S, et al. Multi-modal imaging of tumor cellularity and tryptophan metabolism in human gliomas. *Cancer Imaging*. 2015;15(1):10. doi:10.1186/s40644-015-0045-1 PMID:26245742
- Tan WL, Huang WY, Yin B, Xiong J, Wu JS, Geng DY. Can diffusion tensor imaging noninvasively detect IDH1 gene mutations in astroglomas? A retrospective study of 112 cases. *AJNR*

- Am J Neuroradiol.* 2014;35(5):920–927. doi:10.3174/ajnr.A3803 PMID:24557705
27. Xiong J, Tan WL, Pan JW, et al. Detecting isocitrate dehydrogenase gene mutations in oligodendroglial tumors using diffusion tensor imaging metrics and their correlations with proliferation and microvascular density. *J Magn Reson Imaging.* 2016;43(1):45–54. doi:10.1002/jmri.24958 PMID: 26016619
 28. Xiong J, Tan W, Wen J, et al. Combination of diffusion tensor imaging and conventional MRI correlates with isocitrate dehydrogenase 1/2 mutations but not 1p/19q genotyping in oligodendroglial tumours. *Eur Radiol.* 2016; 26(6):1705–1715. doi:10.1007/s00330-015-4025-4 PMID: 26396108
 29. White ML, Zhang Y, Yu F, Jaffar Kazmi SA. Diffusion tensor MR imaging of cerebral gliomas: evaluating fractional anisotropy characteristics. *AJNR Am J Neuroradiol.* 2011;32(2): 374–381. doi:10.3174/ajnr.A2267
 30. Liu X, Tian W, Kolar B, et al. MR diffusion tensor and perfusion-weighted imaging in preoperative grading of supratentorial nonenhancing gliomas. *Neuro Oncol.* 2011;13(4): 447–455. doi:10.1093/neuonc/noq197
 31. Wang Q, Zhang J, Xu X, Chen X, Xu B. Diagnostic performance of apparent diffusion coefficient parameters for glioma grading. *J Neurooncol.* 2018;139(1):61–68. doi:10.1007/s11060-018-2841-5
 32. Shakir T, Fengli L, Chenguang G, Chen N, Zhang M, Shaohui M. ¹H-MR Spectroscopy in grading of cerebral glioma: a new view point, MRS image quality assessment. *Acta Radiol Open.* 2022;11(2):20584601221077068. doi:10.1177/20584601221077068 PMID:35237448
 33. Barajas RF, Chang JS, Segal MR, et al. Differentiation of recurrent glioblastoma multiforme from radiation necrosis after external beam radiation therapy with dynamic susceptibility-weighted contrast-enhanced perfusion MR imaging. *Radiology.* 2009;253(2):486–496.